Phys. Rev. Lett. 108 (2012)

Designing electrical contacts to MoS_2 monolayers: A computational study

Igor Popov,[1] Gotthard Seifert,[2] and David Tománek[3,*]

[1]*School of Physics and CRANN, Trinity College Dublin 2, Ireland*
[2]*Physikalische Chemie, Technische Universität Dresden, D-01062 Dresden, Germany*
[3]*Physics and Astronomy Department, Michigan State University, East Lansing, Michigan 48824-2320, USA*

(Dated: March 1, 2012)

Studying the reason, why single-layer molybdenum disulfide (MoS_2) appears to fall short of its promising potential in flexible nanoelectronics, we found that the nature of contacts plays a more important role than the semiconductor itself. In order to understand the nature of MoS_2/metal contacts, we performed *ab initio* density functional theory calculations for the geometry, bonding and electronic structure of the contact region. We found that the most common contact metal (Au) is rather inefficient for electron injection into single-layer MoS_2 and propose Ti as a representative example of suitable alternative electrode materials.

PACS numbers: 73.40.Ns, 73.20.At, 73.22.-f, 81.05.Hd

Contrary to popular perception, contacts often play a more crucial role in nanoscale electronics than the semiconducting material itself[1, 2]. Whereas contacts in Si-based devices are no longer considered a problem after many decades of optimization, engineering optimum contacts to electronic nano-devices consisting of silicon[3] or carbon (e.g. nanotubes or graphene)[1, 4] has become a major challenge for the field. More recently, the layered molybdenum disulphide (MoS_2) compound, which is structurally very flexible, has emerged as a promising alternative to silicon-based, carbon-based, and molecular electronics[5, 6]. Bulk MoS_2, a well-established low-cost lubricant, has an indirect band gap of 1.2 eV[7] and a rather high carrier mobility[8, 9]. In contrast to the bulk material, the observed electron mobility in single-layer MoS_2 is unexpectedly low[5, 10].

Here we propose that the observed low electron mobility in MoS_2 may not represent an intrinsic property of the semiconducting single layer, but was possibly biased by unfavorable contacts, which can dominate the electronic characteristics of MoS_2-based nano-electronic devices. Our *ab initio* density functional theory (DFT) calculations for the electronic structure of MoS_2/metal contacts indicate that Au, the most common contact metal in this system[5], forms a tunnel barrier at the interface, which suppresses electron injection into MoS_2. This is possibly the true reason, why the observed carrier mobility in single-layer MoS_2 is lower than expected[5, 10].

Searching for better contacts than provided by Au, we focussed on metals with a low work function that would efficiently inject electrons into the conduction band of MoS_2. Among transition metals with d orbitals that may favorably mix with the Mo4d states, we identified Sc, Ti and Zr as suitable candidates. Among these, Sc and Zr are less suitable due to a large lattice mismatch, and Ti emerges as an ideal candidate with only 1% mismatch to MoS_2. As we will show, the MoS_2/Ti interface displays a much higher density of delocalized states at E_F than the MoS_2/Au contact. Similar to Au, Ti fulfills also other criteria required of a good contact material in electronics, such as high conductivity and chemical, thermal and electrical stability. Therefore, Ti is being used widely as a contact metal in modern microelectronics.

Our DFT calculations use the Perdew-Burke-Ernzerhof form of the exchange-correlation functional[11], as implemented in the SIESTA code[12]. A similar approach had been successfully used to characterize transition metal chalcogenide nanowires[13, 14] and their contacts to metal electrodes[15]. The behavior of valence electrons was described by norm-conserving Troullier-Martins pseudopotentials [16] with partial core corrections. We used a double-zeta basis, including initially unoccupied Mo5p orbitals. The Brillouin zone of the periodic array of MoS_2/metal slabs, separated by a 33 Å vacuum region, was sampled by a $8\times16\times1$ $k-$point grid. We limited the range of the localized orbitals in such a way that the energy shift caused by their spatial confinement was no more than 140 meV[17]. The charge density and potentials were determined on a real-space grid with a mesh cutoff energy of 200 Ry, which was sufficient to achieve a total energy convergence of better than 0.1 meV/unit cell during the self-consistency iterations.

The supercell geometry of the relaxed commensurate contact region between MoS_2 and the close-packed surfaces of Au and Ti is shown in Figs. 1(a) and 1(b). We have represented the metal surfaces by 6-layer slabs. The single-layer MoS_2 consists of a molybdenum monolayer sandwiched between two sulfur monolayers. In each unit cell we distinguish between two types of S atoms: two S atoms are located in the on-top site and six S atoms in the hollow site of the metal substrate. When optimizing this structure using the conjugate gradient technique, all atoms except the bottom four layers of the metal slabs were allowed to relax. In principle, the precise geometry at the metal-semiconductor interface may be affected by our choice of the exchange-correlation functional, which does not describe dispersive

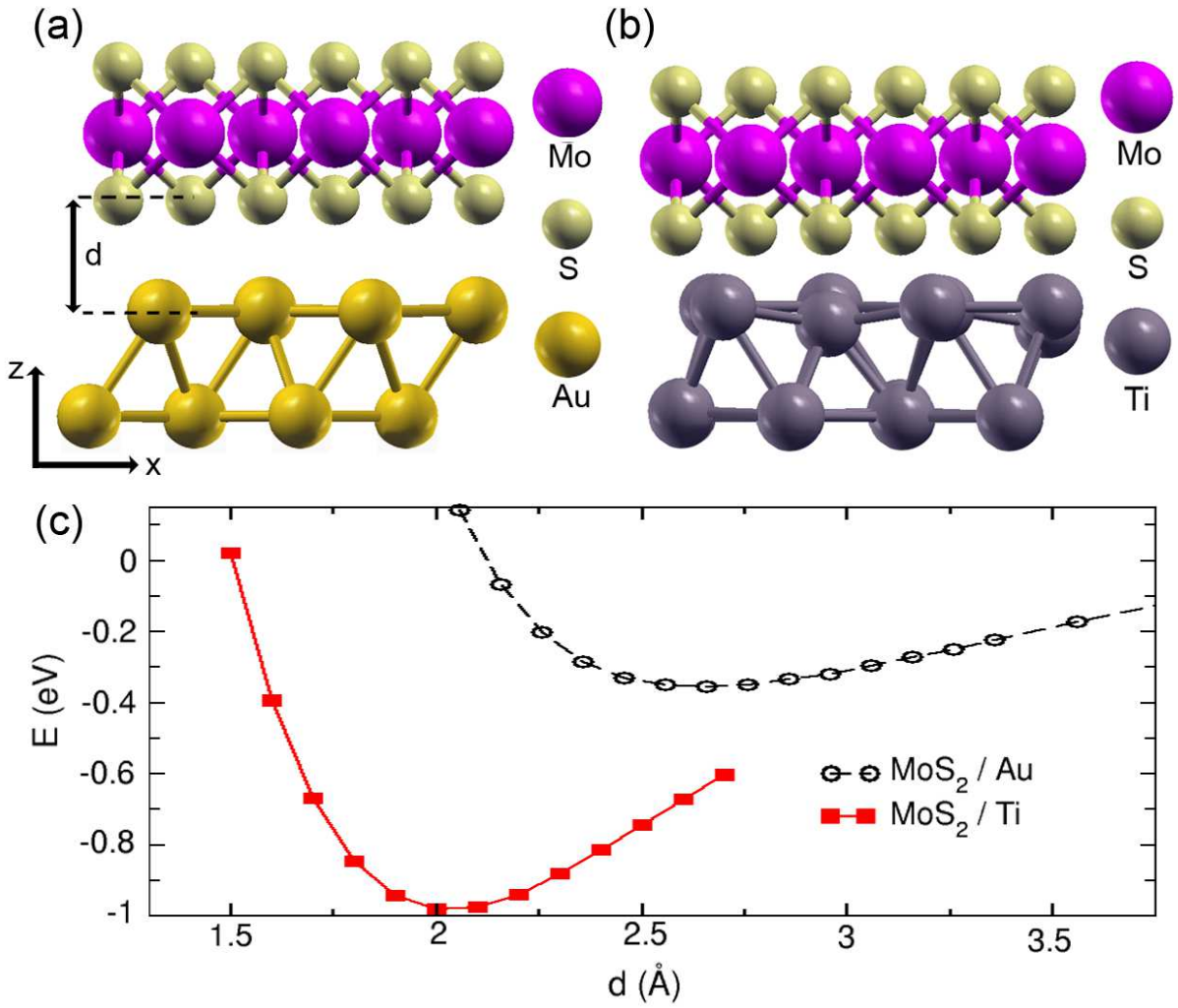

FIG. 1: (Color online) Side view of the relaxed contact region at the interface between MoS_2 and the (a) Au(111) and (b) Ti(0001) surface. (c) Binding energy E per interface metal atom as a function of the separation d between between MoS_2 and the Ti(0001) and Au(111) surface.

interactions accurately. Since the interface bonds are either semi-covalent or covalent and contain in our estimate only $\lesssim$20% van der Waals character, we expect the optimized geometry to be adequate for our study. We noticed that the relaxation within the MoS_2 structure after contacting the metals was very small.

The following major factors determine the electronic transparency of contacts: favorable interface geometry and bonding, the electronic density of states, and the potential barrier at the interface. Strong interconnects are especially important when contacting flexible semiconductors such as MoS_2, which is known to form both planar and tubular nanostructures[18]. Favorable geometry precludes a small lattice mismatch at the interface, and should maximize the overlap between the states at both sides of the interface. The density of states (DOS) at the Fermi level (E_F) should be large throughout the interface region, forming delocalized states with low effective electron mass in order to efficiently transfer electrons between the metal and the semiconductor. The potential barrier at the interface should be as narrow and low as possible to maximize current injection. In the following, we analyze each of these factors for the interface between MoS_2 and Au and Ti as contact metals. As will become clear in the following, Ti turns out to be superior to the commonly used Au as a contact metal.

Contrary to chemically not saturated sulfur, which forms favorable thio bonds to Au, the sulfur in MoS_2 is fully saturated and does not bond strongly to Au. This is reflected in the fact that the shortest distance of 2.62 Å between S in the on-top site and the Au atoms directly underneath is about 0.2 Å longer than the sum of the S and Au covalent radii. The distance between the S atoms in the hollow sites and their closest Au neighbors is significantly

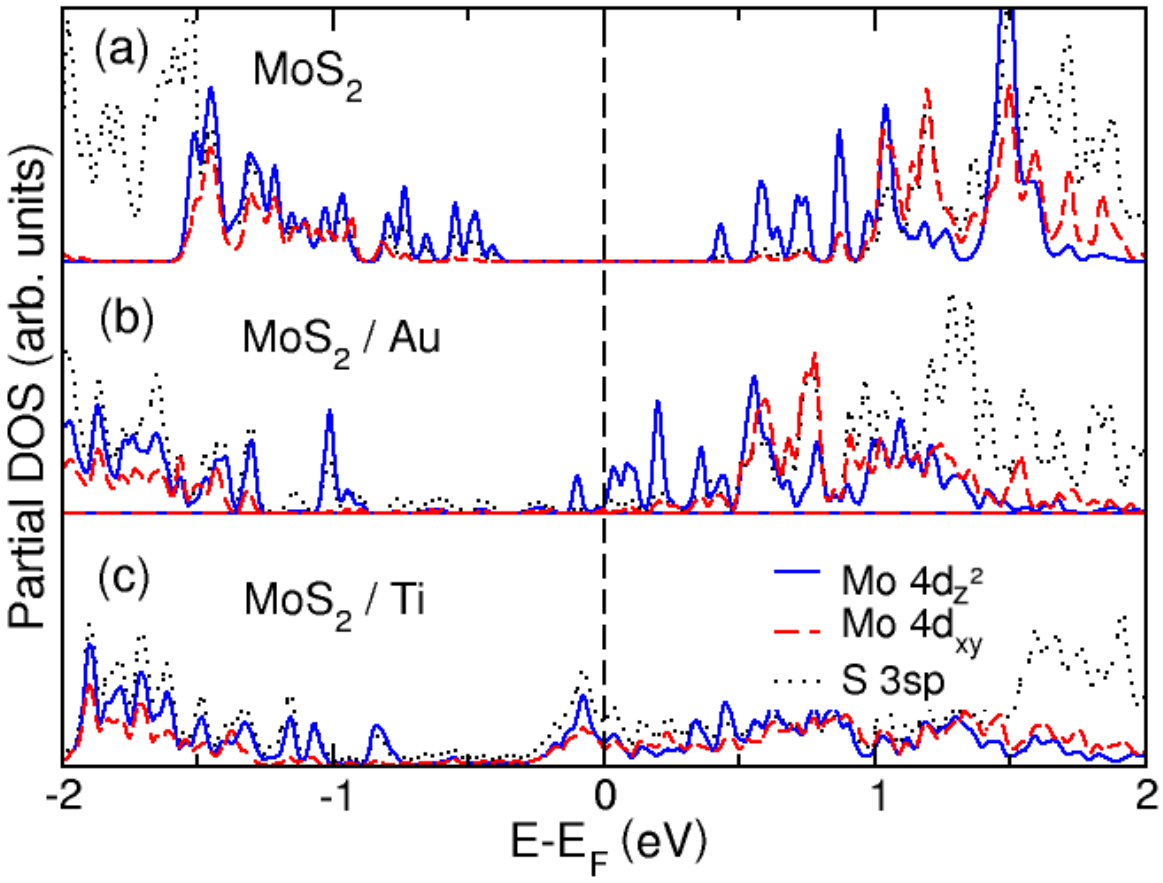

FIG. 2: (Color online) Partial electronic density of Mo and S states, which are relevant to bonding and charge injection, in (a) the single-layer MoS_2, (b) the MoS_2/Au system, and (c) the MoS_2/Ti system. Only a narrow energy region around the Fermi level E_F is shown.

larger, namely 3.15 Å. The average separation between the top layer of Au and the Mo layer is 4.21 Å, large enough to suppress any efficient wavefunction overlap.

When compared to Au, the equilibrium separation between Ti and MoS_2 is much lower. In this case, the majority S atoms, which are in the hollow site, play the key role for adjusting the interlayer separation, trying to replicate the environment of Ti in the stable compound TiS_2. With the equilibrium distance between S atoms at the hollow site and its closest Ti neighbors of 2.54 Å, the optimum separation between MoS_2 and Ti is about 2.0 Å, much shorter than the sum of the Ti and S covalent radii of 2.38 Å. The resulting repulsion between the minority S atoms, which are in the on-top site, pushes away the Ti atoms underneath, reaching an equilibrium distance of 2.34 Å, close to the sum of the respective covalent radii. The average Mo-Ti distance is 3.57 Å, which is 0.64 Å shorter than the Mo-Au distance, indicating favorable conditions for a large wavefunction overlap.

To characterize the contact bond strength, we define the binding energy E between the metal and the MoS_2 layer as the total energy difference between the combined and the isolated systems and display our results in Fig. 1(c). We find that the binding of MoS_2 to Au is considerably weaker than to Ti, with the binding energy per surface metal atom of 0.36 eV in case of Au as compared to 0.98 eV in case of Ti.

The electronic transparency of a contact can be quantified in a quantum transport calculation. For low bias voltages, a suitable approach may involve calculating the equilibrium Green's function, which to a large extent reflects the electronic density of states near E_F and the degree of delocalization of these states within the contact region. For a detailed insight into the reason, why some contacts are better than others, we proceed with a careful analysis of these quantities.

The DOS projection onto selected Mo and S orbitals is presented in Fig. 2 for the single-layer MoS_2, MoS_2/Au and MoS_2/Ti. The bottom of the conduction band and the top of the valence band of the single-layer MoS_2 is dominated

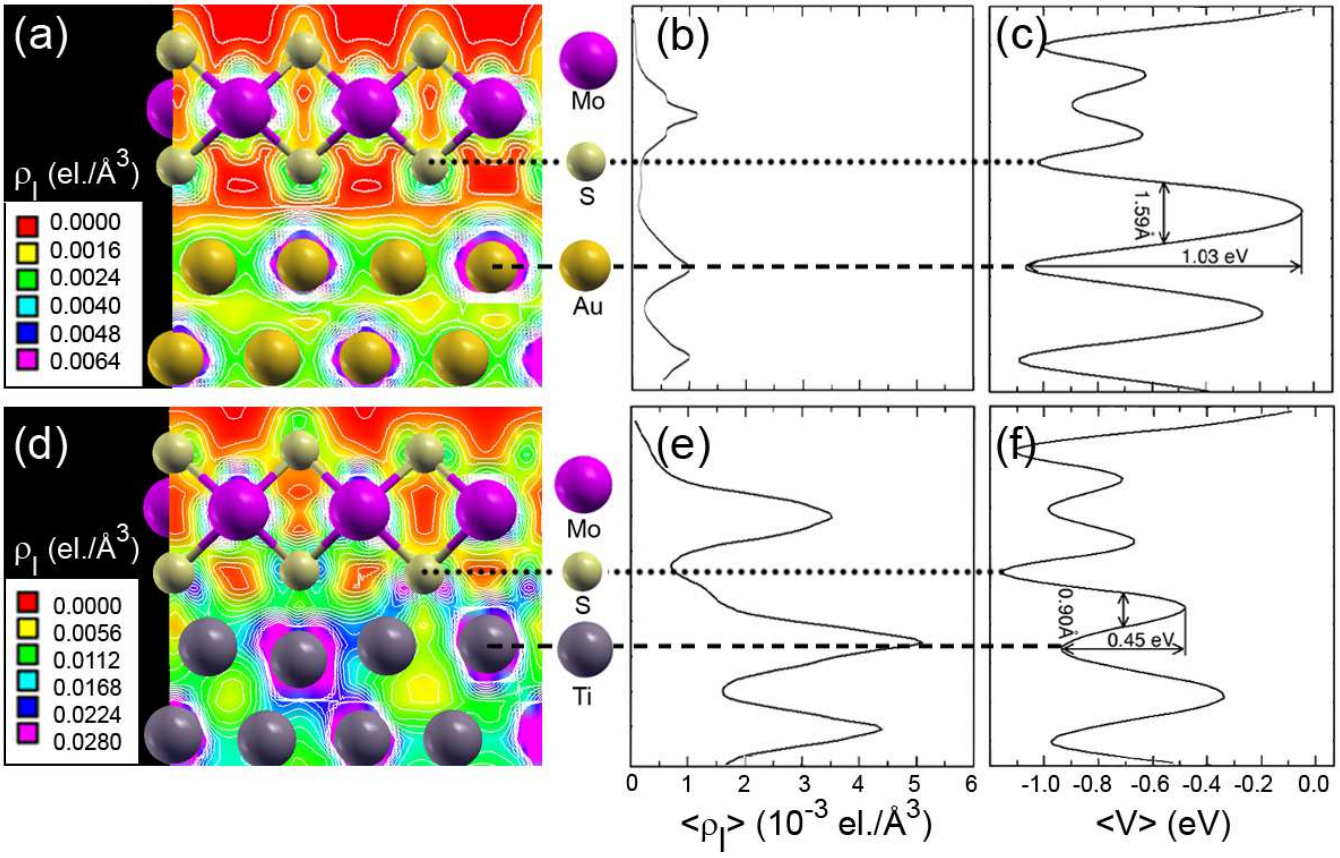

FIG. 3: (Color online) Electronic structure at the interface between MoS_2 and (a-c) Au and (d-f) Ti. Contour plots of the charge density ρ_l associated with states in the energy range $E_F - 0.1$ eV$< E < E_F + 0.1$ eV in planes normal to the interface in (a) MoS_2/Au and (d) MoS_2/Ti. Average value of $< \rho_l > (z)$ in planes parallel to the interface of (b) MoS_2/Au and (e) MoS_2/Ti. Average electrostatic potential $<V_l> (z)$ in planes normal to the interface in (c) MoS_2/Au and (f) MoS_2/Ti. The dotted line in the panels indicates the location of the sulfur layer closest to the metal and the dashed line the position of the topmost metal layer.

by Mo4d_{z^2} states, with the other Mo states playing a minor role. Since the work function $\Phi(MoS_2) = 5.2$ eV is larger than that of most metals, the electronic transparency of the contact is maximized when electronic states at the Fermi level of the contact metal align and strongly overlap with the Mo4d_{z^2} states near the bottom of the conduction band.

As seen in Fig. 2(b), upon making contact with Au, the MoS_2/metal interface becomes metallic. The Fermi level of the combined system shifts upwards, to about 0.1 eV above the bottom of the conduction band of MoS_2. The states near E_F display dominant Mo4d_{z^2} character with only a small admixture of S3sp states. Consequently, electron injection into the semiconductor will involve primarily the Mo4d_{z^2} states that, according to Fig. 2(b), display a low partial DOS at E_F. The corresponding low carrier density near E_F of the interface is depicted in Fig. 3(a) and Fig. 3(b).

As seen by comparing Fig. 2(b) for MoS_2/Au and Fig. 2(c) for MoS_2/Ti, Ti as contact metal modifies the electronic states near E_F much more than Au. In the MoS_2/Ti system, the Fermi level is shifted upwards, to 0.25 eV above the bottom of the MoS_2 conduction band. This is much higher than in the Au system and causes an increase in the DOS at E_F. The most striking difference to Au is a significant contribution of S3sp and Mo4d_{xy} states near the Fermi level, which is associated with a strong S-Ti mixing. The contribution of Mo4d_{xy} states at E_F is nearly equal to that of the Mo4d_{z^2} states. The broadening of the peaks in the DOS near E_F reflects an increase in the dispersion of the corresponding bands and suggests the formation of delocalized states at the interface.

The character of the states, which determine the low-bias transport, is represented by the density $\rho_l(\mathbf{r})$ of the corresponding carriers in the left panels of Fig. 3(a) for MoS_2/Au and Fig. 3(d) for MoS_2/Ti. As seen in Fig. 3(a), which shows a detailed contour plot of ρ_l, and Fig. 3(b), representing the average $< \rho_l > (z)$ in planes parallel to the interface, the charge carrier density in the interface region between MoS_2 and Au is very low. Consequently, the electron transport across the MoS_2/Au contact is mainly of tunneling nature. Since according to Fig. 2(b) the

electron injection into the MoS_2 layer proceeds exclusively via the Mo4d_{z^2} states, the tunnel barrier from Au to MoS_2 is very wide.

In striking contrast to the MoS_2/Au interface, the charge carrier density in the interface region between MoS_2 and Ti is much larger. This is seen especially when comparing the averaged carrier density $< \rho_l >$ in planes parallel to the interface in Fig. 3(b) for MoS_2/Au and Fig. 3(e) for MoS_2/Ti. Of particular interest is the difference between the electron density at the interfacial sulfur layer, denoted by the dotted line in Fig. 3. The nearly vanishing value of $< \rho_l >$ at this location in MoS_2/Au increases by an order of magnitude in MoS_2/Ti, thus turning tunneling into resonant transport. The carrier density delocalization in MoS_2/Ti, anticipated above due to the DOS broadening, corresponds to a metallization of the interface. This in turn enables direct charge injection into the MoS_2 layer, for which the actual distance between Mo and Ti atoms becomes irrelevant.

In order to complete the analysis of the contacts, we investigate the electrostatic potential regarding the existence of barriers at the metal-semiconductor interface and show the results in Fig. 3(c) for MoS_2/Au and Fig. 3(f) for MoS_2/Ti. Since we observe not only a net charge transfer across the metal-semiconductor interface, but also changes in the electronic structure due to the covalent interaction, these barriers are not ideal Schottky barriers, but rather more general contact tunnel barriers. We define the height of the contact tunnel barrier as the difference between the averaged potential at the top metal layer, indicated by the dashed line in Fig. 3, and the maximum of the averaged potential between the metal and the neighboring sulfur layer.

As anticipated, the tunnel barrier at the interface between the semiconducting MoS_2 layer and the Au surface, which is shown in Fig. 3(c), is relatively high (1.03 eV) and wide. Since the S states of the bottom MoS_2 layer are nearly absent near E_F in the MoS_2/Au system, the true barrier is even wider than the 1.59 Å value at half-height shown in Fig. 3(c). In this case, tunneling involves direct charge transfer from Au to Mo states across two barriers.

Electron injection from Ti to MoS_2 is completely different. As seen in Fig. 3(f), electrons in this system have to bypass the much lower (0.45 eV) and narrower (0.9 Å) barrier to reach the delocalized states at the MoS_2/Ti interface. In comparison to Au as contact metal, the significant reduction of the barriers at the interface with Ti will significantly improve the electronic transparency of the contact.

Even though Au is commonly believed to be the ideal contact metal to many sulfur-terminated systems including multi-layer MoS_2, our study shows that the opposite is true when contacting single-layer MoS_2. A multi-layer system is preferentially contacted from the side, where Au can bond chemically to not saturated sulfur atoms at the edge. Since contacting a single-layer from the side is insufficient for good electron injection, the preferred geometry is a top contact discussed here. In this scenario, we identified unexpected qualitative differences between different contact metals in the way they inject carriers into MoS_2.

The basic difference is that between an inefficient tunnel contact in MoS_2/Au and a low-resistance ohmic contact providing a direct injection channel in MoS_2/Ti. We discuss MoS_2/Ti only as a representative example of an optimum designer contact that is superior to the state-of-the-art. Good contact metal candidates must, of course, first fulfill macroscopic criteria such as high conductivity and chemical, thermal and electrical stability. Additional criteria for an optimum contact in nanoelectronics, which we find fulfilled in the case of Ti, include a favorable interface geometry and bonding. In terms of electronic structure, an optimum contact has a high density of delocalized states across the interface at the Fermi level of the combined system, corresponding to a minimized or non-existent tunnel barrier between the two materials.

In conclusion, we performed *ab initio* density functional theory calculations of MoS_2/Au and MoS_2/Ti contacts to study the reason, why single-layer molybdenum disulfide appears to fall short of its promising potential in flexible electronics according to recent experiments[5, 10]. We found that the nature of contacts plays a more important role in these systems than the semiconductor itself. Our calculations for the geometry, bonding and electronic structure of the contact region suggest that the most common contact metal (Au) forms a tunnel contact to single-layer MoS_2 and thus is rather inefficient for electron injection. We find that Ti is a suitable alternative as electrode material, since it forms a low-resistance ohmic contact. We also provide specific criteria for selecting materials besides Ti that should optimize the electronic transparency of the contact. Higher contact transparency reduces the required bias voltages for operation and may also improve the frequency response of these structurally flexible electronic devices, which may eventually open new horizons for electronics based on transition metal chalcogenides.

DT was partly supported by the National Science Foundation Cooperative Agreement #EEC-0832785, titled "NSEC: Center for High-rate Nanomanufacturing". GS was partly supported by the European Research Council (ERC - project INTIF 226639). IP was supported by the Science Foundation of Ireland (SFI) and CRANN. Computational resources for this project were provided by the ZIH Dresden and the Trinity College High Performance Computing Center (TCHPC).

* E-mail: tomanek@pa.msu.edu

[1] F. Léonard and A. A. Talin, Phys. Rev. Lett. **97**, 026804 (2006).
[2] Y.-F. Lin and W.-B. Jian, Nano Lett. **8**, 3146 (2008).
[3] U. Landman, R. N. Barnett, A. G. Scherbakov, and P. Avouris, Phys. Rev. Lett. **85**, 1958 (2000).
[4] D. T. N. Nemec and G. Cuniberti, Phys. Rev. Lett. **96**, 076802 (2006).
[5] B. Radisavljevic, A. Radenovic, J. Brivio, V. Giacometti, and A. Kis, Nature Nanotech. **6**, 147 (2011).
[6] Y. Yoon, K. Ganapathi, and S. Salahuddin, Nano Lett. **11**, 3768 (2011).
[7] K. K. Kam and B. A. Parkinson, J. Phys. Chem. **86**, 463 (1982).
[8] R. Fivaz and E. Mooser, Phys. Rev. **163**, 743 (1967).
[9] V. Podzorov, M. E. Gershenson, C. Kloc, R. Zeis, and E. Bucher, Appl. Phys. Lett. **84**, 3301 (2004).
[10] K. S. Novoselov, D. Jiang, F. Schedin, T. J. Booth, V. V. Khotkevich, S. V. Morozov, and A. K. Geim, Proc. Natl. Acad. Sci. USA **102**, 10451 (2005).
[11] J. P. Perdew, K. Burke, and M. Ernzerhof, Phys. Rev. Lett. **77**, 3865 (1996).
[12] J. M. Soler, E. Artacho, J. D. Gale, A. García, J. Junquera, P. Ordejón, and D. Sánchez-Portal, J. Phys. Cond. Matter **14**, 2745 (2002).
[13] I. Popov, T. Yang, S. Berber, G. Seifert, , and D. Tománek, Phys. Rev. Lett. **99**, 085503 (2007).
[14] T. Yang, S. Okano, S. Berber, and D. Tománek, Phys. Rev. Lett. **96**, 125502 (2006).
[15] I. Popov, A. Pecchia, S. Okano, N. Ranjan, A. D. Carlo, and G. Seifert, Appl. Phys. Lett. **93**, 083115 (2008).
[16] N. Troullier and J. L. Martins, Phys. Rev. B **43**, 1993 (1991).
[17] E. Artacho, D. Sánchez-Portal, P. Ordejón, A. García, and J. M. Soler, Phys. Stat. Sol. (b) **215**, 809 (1999).
[18] R. Tenne, L. Margulis, M. Genut, and G. Hodes, Nature (London) **360**, 444 (1992).